

Evidence of komatiitic basalt enclaves in the Téra-Ayorou pluton (Liptako, West Niger) (West African Craton)

Sofiyane Abdourahamane Attourabi

Mallam Mamane Hallarou

Yacouba Ahmed

Département de Géologie,
Laboratoire Eaux Souterraines et Géoressources,
Faculté des Sciences et Techniques,
Université Abdou Moumouni de Niamey, Niger

Mahamane Moustapha Sanda Chékaraou

Département de Didactique des Disciplines, Faculté des Sciences de
l'Éducation, Université Djibo Hamani de Tahoua, Niger

[Doi:10.19044/esj.2024.v20n14p74](https://doi.org/10.19044/esj.2024.v20n14p74)

Submitted: 25 April 2024

Accepted: 28 May 2024

Published: 31 May 2024

Copyright 2024 Author(s)

Under Creative Commons CC-BY 4.0

OPEN ACCESS

Cite As:

Attourabi, S. A., Hallarou, M. M., Ahmed, Y., & Chékaraou, M. M. S. (2024). *Evidence of komatiitic basalt enclaves in the Téra-Ayorou pluton (Liptako, West Niger) (West African Craton)*. European Scientific Journal, ESJ, 20 (14), 74.

<https://doi.org/10.19044/esj.2024.v20n14p74>

Abstract

The present study focuses on the basic enclaves (amphibolo-pyroxenites) of the Téra-Ayorou pluton in Niger Liptako (NE portion of the Man Ridge of the West African Craton). The methodology used includes field observations, supported by polarizing microscope observations of thin sections and geochemical analyses of whole rock. These enclaves are characterized by high MgO, low Na₂O, K₂O, and TiO₂ contents, high CaO/Al₂O₃ ratios, depletion of light rare earth and enrichment in Ni and Cr. These basic enclaves are thought to come from certain basic to ultrabasic Pogwa and Ladanka plutonites in the Diagorou-Darbani greenstone belt, with which they share the same geochemical characteristics. This suggests that these enclaves were ripped out by the pluton as it was being emplaced. The basic enclaves and basic plutonites with ultrabasites have different signatures from those of the birimian basites of the West African Craton, which are tholeiitic and calc-alkaline. The amphibolo-pyroxenite enclaves of the Téra-

Ayorou pluton and the basic to ultrabasic plutonites of the Diagorou-Darbani greenstone belt constitute a fairly continuous line of komatiitic rocks from peridotites (serpentinites) to basalts (metapyroxenites, amphibolites). This komatiitic lineage results from the fractional crystallization of a magmatic liquid from a mantle source with variable partial melting rates. The komatiitic line and the tholeiitic and calc-alkaline lines are closely intertwined in the field.

Keywords: Basic enclaves of Téra-Ayorou Pluton, Niger Liptako, West African Craton, Komatiitic line, Fractional crystallization

Introduction

The Baoulé-Mossi area of the West African Craton is characterized by alternating granitoids and greenstone belts (Grenholm, 2019). These are characterized by a lithostratigraphic succession comprising a volcanic unit at the base and a sedimentary unit at the top (Baratoux et al., 2011, 2015; Grenholm, 2019). Two magmatic lines have been distinguished within the volcanic complex: the tholeiitic line and the calc-alkaline line (Baratoux et al., 2011; Grenholm, 2019). According to the authors, the tholeiitic lineage characterizes an emplacement in a MORB-type oceanic domain (Lompo, 2009), an oceanic shelf area (Poucllet et al., 1996), or an island arc domain (Ama Salah et al., 1996; Soumaila et al., 2004, 2008). The calc-alkaline lineage characterizes an emplacement in a subduction context (Soumaila et al., 2008). Granitoids are essentially composed of TTGs and are intrusive in greenstone belts (Parra-Avila et al., 2017). The granitoids contain numerous basic and ultrabasic enclaves (Machens, 1973). The Téra-Ayorou pluton (Nigerian Liptako), which is the subject of this study, contains numerous enclaves of amphibolites, pyroxenites, and amphibolo-pyroxenites. These enclaves have not previously been the subject of any detailed, in-depth study. The aim of this study is to determine the petrography, geochemistry and magmatic lineage of these enclaves.

Geological context

The West African Craton is made up of two ridges, the Réguibat ridge to the north and the Léo-Man ridge to the south (Figure 1), each comprising an Archaean western province dated at 3.5 to 2.7 Ga (Kouamelan et al., 2015; Rollinson, 2016) and an eastern Birimian province dated at 2.7 to 1.96 Ga (Grenholm, 2019).

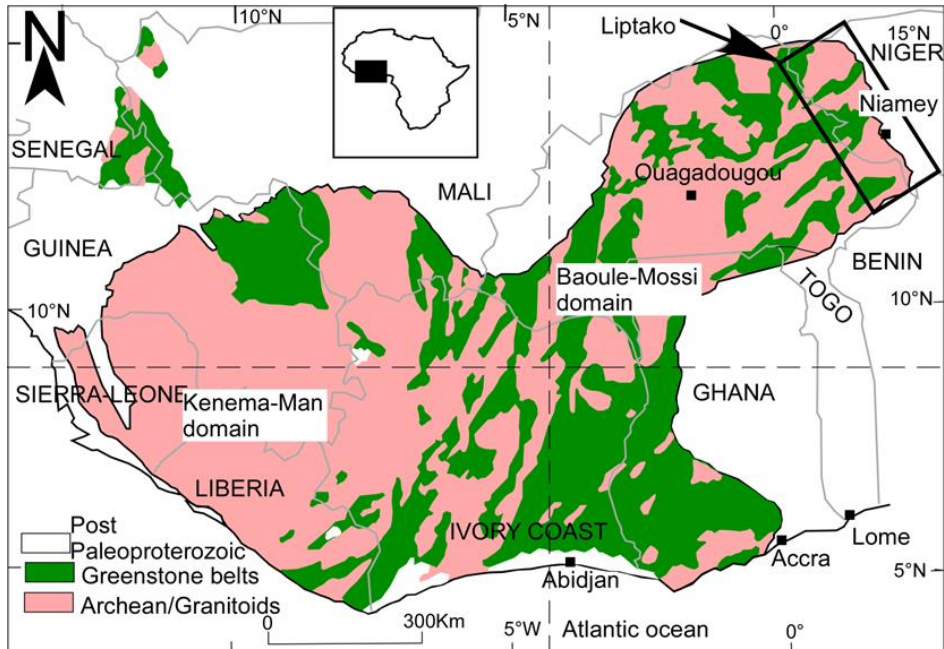


Figure 1: Synthetic geological map of the Man Ridge (from Milési et al., 1989)

The Niger Liptako corresponds to the north-eastern (NE) edge of the Léo-Man ridge (Figure 1). It is characterized by alternating greenstone belts (Gorouol, Diagorou-Darbani, Sirba, and Makalondi) and granitoid plutons (Téra-Ayorou, Dargol-Gothèye, and Torodi) trending broadly NE-SW (Ahmed et al., 2022) (Figure 2). The geological formations in the greenstone belts are metabasalts, amphibolites, ultramafic and mafic intrusive units, often transformed into talcschists and chloritoschists, detrital sediments with little metamorphism, and small volumes of plutonic and volcanic rocks with intermediate to acidic chemistry (Ama Salah et al., 1996; Soumaila et al., 2004; Garba Saley et al., 2021; Hallarou, 2021). Granitoids are mainly composed of TTGs (tonalite, trondhjemite, granodiorite) (Pons et al., 1995).

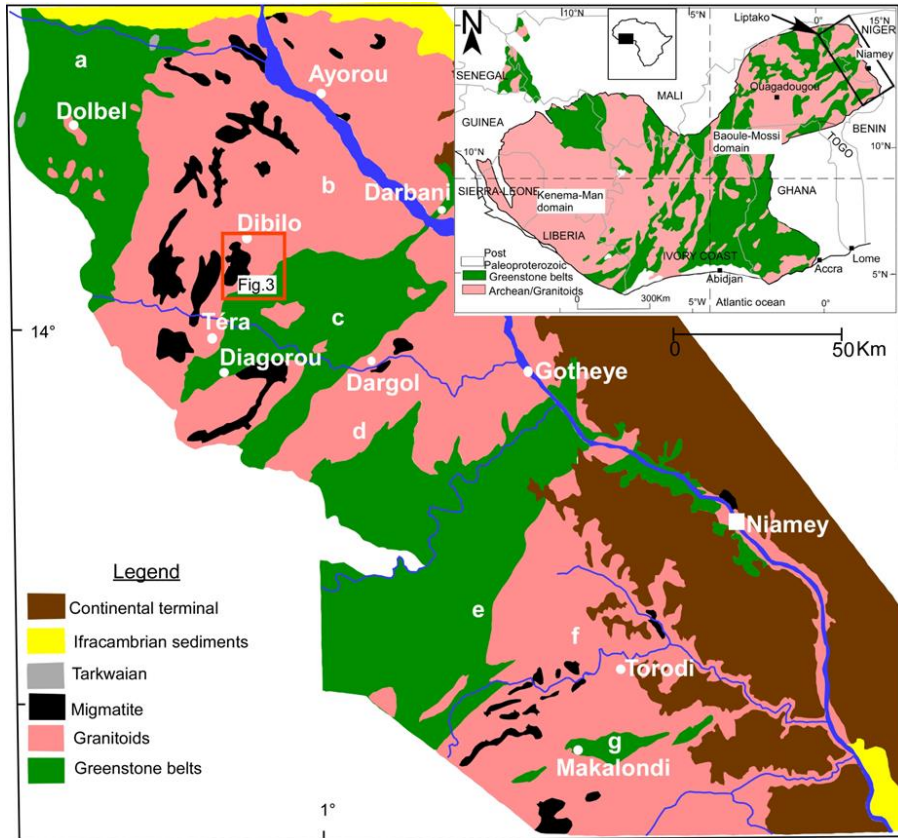


Figure 2: Simplified geological map of Liptako (Machens, 1973; Dupuis et al., 1991, modified). a: Goroual greenstone belt; b: Pluton of Téra-Ayorou; c: Diagorou-Darbani greenstone belt; d: Pluton of Dargol-Gothèye; e: Sirba greenstone belt; f: Pluton of Torodi; g: Makalondi greenstone belt

The Téra-Ayorou pluton is located in the northern part of the Nigerian Liptako. It is a syn to late-tectonic pluton emplaced during the Paleoproterozoic (U-Pb and K-Ar dating: $2158 \text{ Ma} \pm 9$ (Lama, 1993; Cheilletz et al., 1994). The geology of this pluton is represented by migmatites, granodiorites, and calc-alkaline biotite- or 2 micas-bearing granites, with enclaves of amphibolite and pyroxenite (Machens, 1973; Pons et al., 1995). These formations are intersected by veins of quartz and pegmatites (Attourabi et al., 2021; Ahmed et al., 2022) and late dolerites (Noura et al., 2023a) (Figure 3).

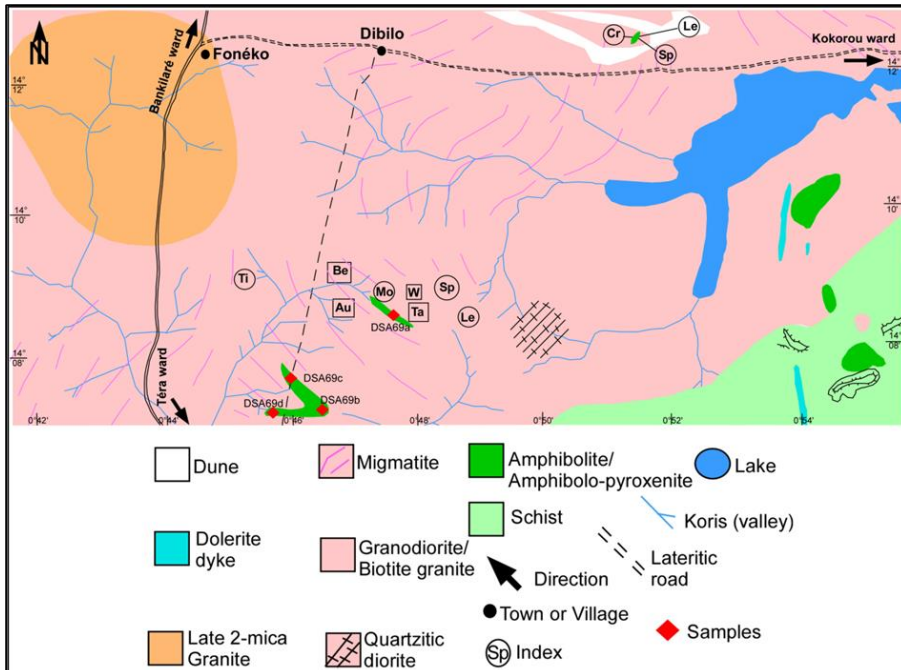


Figure 3: Simplified geological map of Dibilo (Machens, 1961; Attourabi et al., 2021; Ahmed et al., 2022)

Methodology

The methodology used for this study consisted of fieldwork and laboratory work. The fieldwork consisted of a petrographic description of the enclaves and sampling.

The laboratory work involved making 3 thin sections (DSA69b, DSA69c, DSA69d) at the "Centre de Recherche Géologique et Minière" (CRGM) in Niger, and their observations in unanalyzed polarised light (LPNA), analyzed polarised light (LPA) and reflected light using a LEICA DM2700 microscope equipped with five $\times 5$, $\times 10$, $\times 20$, $\times 50$, $\times 100$ magnification objectives and an image capture device connected with computer. These observations were made at the Georesources Laboratory in the Geology Department of the Abdou Moumouni University in Niamey.

One sample (DSA69a) was analyzed at the "Service d'Analyse des Roches et Minéraux (SARM)" of the "Centre de Recherches Pétrographiques et Géochimiques (CRPG)" in Nancy, France. Major element (SiO_2 , Al_2O_3 , Fe_2O_3 , MnO , MgO , CaO , Na_2O , K_2O , TiO_2 , P_2O_5 , PF, Total) values were obtained by ICP-OES (Inductively Coupled Plasma-Optical Emission Spectrometry) with a Thermo Fischer iCap6500 and trace element and rare earth element (As, Ba, Be, Bi, Cd, Co, Cr, Cs, Cu, Ga, Ge, Hf, In, Mo, Nb, Ni, Pb, Rb, Sb, Sc, Sn, Sr, Ta, Th, U, V, W, Y, Zn, Zr, La, Ce, Pr, Nd, Sm, Eu, Gd, Tb, Dy, Ho, Er, Tm, Yb, Lu, Li) values were obtained by ICP-MS

(Inductively Coupled Plasma-Mass Spectrometry) and ICP-OES with a Thermo Fischer iCap6500. The geochemical diagrams were produced using GCDkit 6.1_for R.4.1.3 software (Janoušek et al., 2006).

Results and Discussion

Petrography

In the study area (Téra-Ayorou granitoid pluton), enclaves of greenstone belts were observed to the south of Dibilo, to the south of Fonéko, to the south of Kokorou and to the west part of Téra. These enclaves are represented by amphibolo-pyroxenites. The rock is blackish and shows an $N10^{\circ}$ to $N20^{\circ}$ foliation. This foliation is marked by alternating dark beds (amphibole or pyroxene) and light beds (feldspar) (Figure 4). These enclaves are intersected by quartz veins running N-S and $N130^{\circ}$.

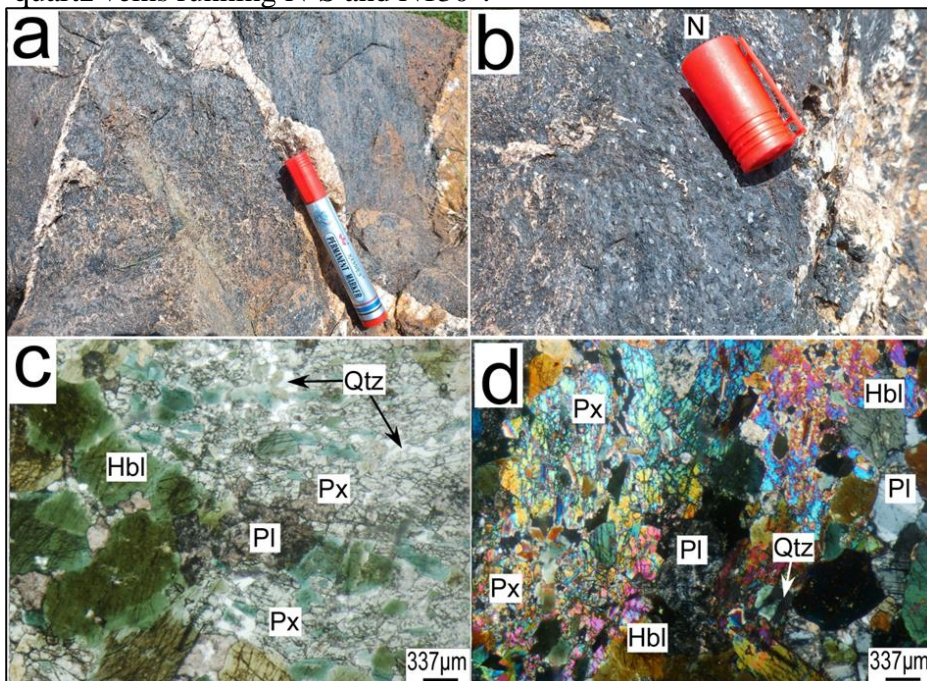


Figure 4: Amphibolo-pyroxenite enclaves crossed by quartz veins south of Dibilo. (c, d, e and f) LPNA and LPA microphotographs of the enclave showing the mineralogical association: Hornblende (Hbl), Pyroxene (Px), Plagioclase (Pl), and Quartz (Qtz)

Microscopically, amphibopyroxenites have a granoblastic texture. They are composed of quartz, plagioclase, amphibole (hornblende), and pyroxene (Figure 4). Quartz is present in the form of large mono and/or polycrystalline patches or as small interstitial crystals. It sometimes forms rectilinear inclusions in the poeciloblasts of hornblende. Plagioclase is strongly sericitised and occurs as automorphous, mottled crystals (polysynthetic twins), or as microcrystals included in the poeciloblasts of

hornblende. Amphibole is green hornblende. It occurs as pleochroic automorphic crystals in green hues (in LPNA). Hornblende sometimes has one cleavage plane (longitudinal section) or two cleavages (transverse section). In the elongated section, extinction occurs obliquely to the cleavage plane. Pyroxene occurs in the form of orthopyroxene crystals, which are largely uralitized.

Discussion

The amphibole-pyroxenite enclave studied is characterized by a high MgO content (11.60 wt%) (Figure 5a), low alkali (Na₂O: 1.43 wt%; K₂O: 0.72 wt%) and TiO₂ (0.61 wt%) (Figure 5b), a high CaO/Al₂O₃ ratio (1.6) and a depletion in light rare earth and an absence of Eu anomalies (Figure 6a), with negative anomalies in Th, Nb and positive in Pb and U (Figure 6b) (Table 1).

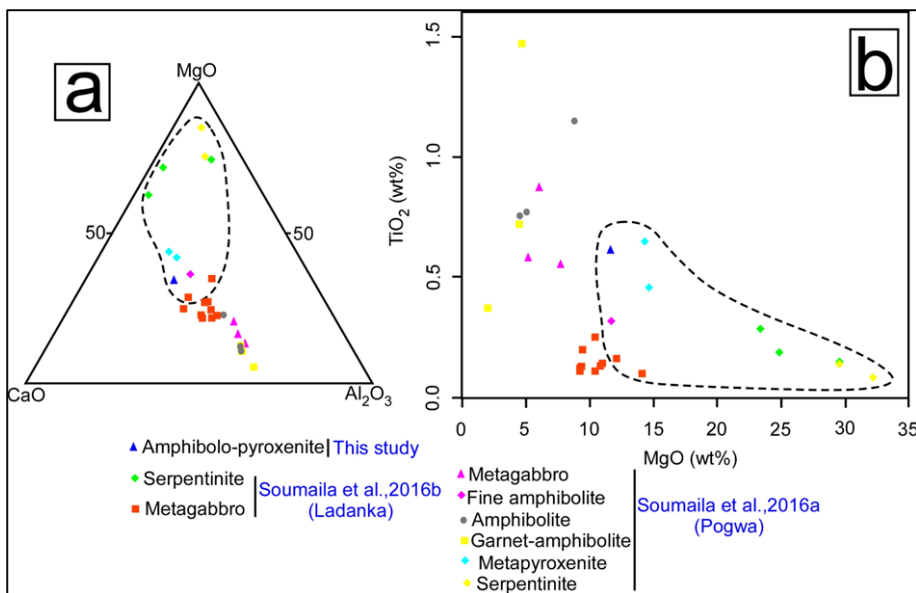


Figure 5: Projection of the amphibolo-pyroxenite enclave of the Téra-Ayorou (this study) and the basic to ultrabasic plutonites of the Diagorou-Darbani belt (Soumaila et al., 2016a, 2016b) in the diagrams of Blais et al. (1977): (a) CaO-MgO-Al₂O₃; (b) MgO vs TiO₂.

Table 1: Majors and trace elements analyses of the Pogwa Rocks (Soumaila et al.,2016a) and the Tera-Ayorou enclaves (this study)

| Soumaila et al., 2016a | | | | | | | | | | | | | | | This study |
|--------------------------------|-----------|--------|------------|--------|-------|------------|--------|-------|-----------------|--------|--------|----------|------------|-------|------------|
| Rocks | Metapyrox | | Metagabbro | | | Grt-AmphPg | | | Grt free AmphPg | | | F-AmphPg | Ultrabasic | | Am-Px |
| Samples | Fpd-21 | Fpd-21 | Fpd-3 | Fpd-22 | Fpd-4 | Fpd-5 | Fpd-13 | Fpd-7 | Fpd-17 | Fpd-18 | Fpd-20 | Fpd-12 | Th738 | Th538 | DSA69a |
| SiO ₂ | 49,36 | 50,42 | 45,45 | 46,46 | 44,57 | 49,39 | 43,66 | 44,79 | 45,38 | 44,54 | 45,63 | 55,52 | 39,63 | 44,46 | 47,21 |
| Al ₂ O ₃ | 7,81 | 6,63 | 19,45 | 20,45 | 23,06 | 26,4 | 21,95 | 24,18 | 23,48 | 17,62 | 23,31 | 9,5 | 3,14 | 5,78 | 8,85 |
| Fe ₂ O ₃ | 1,31 | 1,34 | 1,02 | 1,02 | 0,79 | 0,45 | 1,28 | 0,92 | 0,92 | 1,28 | 0,94 | 0,97 | 1,25 | 0,98 | 13,39 |
| MnO | 0,21 | 0,24 | 0,13 | 0,12 | 0,08 | 0,06 | 0,17 | 0,1 | 0,1 | 0,16 | 0,11 | 0,18 | 0,18 | 0,15 | 0,29 |
| MgO | 14,35 | 14,66 | 7,67 | 5,97 | 5,13 | 2,05 | 4,69 | 4,49 | 4,47 | 8,77 | 4,95 | 11,7 | 32,19 | 29,5 | 11,60 |
| CaO | 12,06 | 12,12 | 11,72 | 11,88 | 12,53 | 13,15 | 12,33 | 13,59 | 13,41 | 12,11 | 13,19 | 11,05 | 2,57 | 4,23 | 13,83 |
| Na ₂ O | 0,81 | 0,76 | 2 | 2,4 | 2,12 | 2,57 | 2,04 | 2,08 | 2 | 1,62 | 2,04 | 1,37 | 0,19 | 0,05 | 1,43 |
| K ₂ O | - | - | 0,51 | 0,11 | 1,07 | - | - | - | - | 0,13 | 0,05 | 0,09 | 0 | 0 | 0,72 |
| TiO ₂ | 0,65 | 0,46 | 0,55 | 0,87 | 0,58 | 0,37 | 1,47 | 0,72 | 0,76 | 1,15 | 0,77 | 0,32 | 0,09 | 0,14 | 0,61 |
| P ₂ O ₅ | 0,06 | 0,09 | 0,06 | 0,16 | 0,09 | 0,16 | 0,25 | 0,16 | 0,12 | 0,05 | 0,08 | 0,05 | 0,07 | 0,05 | 0,15 |
| Total | 98,58 | 99,87 | 98,93 | 99,85 | 99,87 | 99,83 | 99,89 | 99,81 | 99,68 | 99,85 | 100,1 | 100,4 | 98,99 | 99,43 | 99,31 |
| Ba | 33,26 | 22,24 | 139,9 | 77,25 | 449,6 | 112,4 | 128 | 54,61 | 86,36 | 74,21 | 72,98 | 138,7 | 9,5 | 0,9 | 70,43 |
| Ce | 18,56 | 22,6 | 8,5 | 21,76 | 8,76 | 18,48 | 22,19 | 15,27 | 14,8 | 16,09 | 14,97 | 14,86 | 1,04 | 0,66 | 11,28 |
| Co | 53,98 | 58,51 | 39,78 | 36,59 | 35,56 | 12,4 | 33,78 | 29,36 | 27,68 | 54,91 | 30,39 | 47,09 | 117 | 83,9 | 82,75 |
| Cr | 1499 | 743,7 | 198,9 | 154,1 | 198,9 | 154,1 | 19,16 | 49,09 | 9,94 | 20,24 | 107 | 1175 | 3285 | 2940 | 2202,34 |
| Dy | 3,39 | 2,72 | 1,72 | 3,92 | 1,72 | 3,92 | 1,55 | 2,18 | 5,81 | 3,49 | 3,4 | 1,61 | 0,36 | 0,5 | 1,90 |
| Er | 1,8 | 1,48 | 0,95 | 2,11 | 0,95 | 2,11 | 0,87 | 1,18 | 3,39 | 1,94 | 1,87 | 0,95 | 0,23 | 0,29 | 1,09 |
| Eu | 1,02 | 0,82 | 0,8 | 1,57 | 0,85 | 1,21 | 1,68 | 1,25 | 1,16 | 1,25 | 1,24 | 0,58 | 0,08 | 0,09 | 0,69 |
| Gd | 3,79 | 3,21 | 1,87 | 4,62 | 1,76 | 2,56 | 5,84 | 3,71 | 3,88 | 4,26 | 3,69 | 1,82 | 0,33 | 0,29 | 1,87 |
| Hf | 1,07 | 1,05 | 0,59 | 1,23 | 0,59 | 0,75 | 1,32 | 0,9 | 1,02 | 1,21 | 0,89 | 0,97 | 0,16 | 0,18 | 1,35 |
| Ho | - | - | - | - | - | - | - | - | - | - | - | - | - | - | 0,40 |
| La | 0,53 | 6,53 | 3,28 | 7,46 | 3,58 | 8,34 | 7,16 | 5,19 | 5,43 | 4,93 | 5,26 | 8,34 | 0,45 | 0,24 | 4,42 |
| Lu | 0,25 | 0,24 | 0,13 | 0,3 | 0,12 | 0,17 | 0,51 | 0,26 | 0,29 | 0,32 | 0,26 | 0,16 | 0,04 | 0,06 | 0,17 |
| Nb | 2 | 2,46 | 0,99 | 2,45 | 0,98 | 1,75 | 4,74 | 1,7 | 1,79 | 1,82 | 1,87 | 1,45 | 0,13 | 0,17 | 3,37 |

| | | | | | | | | | | | | | | | |
|----|-------|-------|-------|-------|-------|-------|-------|-------|-------|-------|-------|-------|------|------|--------|
| Nd | 15,77 | 17,82 | 6,9 | 18,72 | 6,71 | 12,08 | 20,28 | 13,79 | 13,22 | 15,35 | 13,65 | 9,74 | 0,69 | 0,58 | 7,75 |
| mg | - | - | - | - | - | - | - | - | - | - | - | - | - | - | - |
| Ni | 116,3 | 127,3 | 91,49 | 81,1 | 29,74 | 25,74 | 6,2 | 7,8 | 6,58 | 22,64 | 45,44 | 66,2 | 1229 | 1234 | 592,94 |
| Pb | - | - | 2,24 | 2,2 | 2,88 | 3,79 | 2,16 | 2,63 | 2,62 | - | 3,01 | 8,88 | 0,47 | 0,26 | 2,57 |
| Pr | 3,14 | 3,9 | 1,33 | 3,68 | 1,33 | 2,65 | 3,86 | 2,62 | 2,51 | 2,93 | 2,61 | 2,33 | 0,19 | 0,12 | 1,73 |
| Rb | 1,47 | 1,28 | 16,84 | 3,23 | 32,46 | 1,07 | 0,75 | 0,72 | 2,14 | 1,74 | 2,41 | 1,78 | 1,27 | 0,72 | 7,30 |
| Sm | 4,14 | 3,89 | 1,91 | 4,94 | 1,83 | 2,9 | 5,61 | 3,92 | 3,86 | 4,35 | 3,81 | 2,09 | 0,2 | 0,25 | 1,98 |
| Sr | 90,95 | 49,1 | 516,5 | 559,7 | 747,5 | 685,6 | 524,4 | 612,7 | 546,5 | 294,7 | 507,1 | 282,8 | 13,3 | 20,5 | 245,62 |
| Ta | 0,12 | 0,12 | 0,07 | 0,14 | 0,07 | 0,13 | 0,27 | 0,1 | 0,12 | 0,11 | 0,12 | 0,1 | 0,01 | 0,02 | 0,31 |
| Tb | 0,57 | 0,47 | 0,29 | 0,67 | 0,27 | 0,38 | 0,92 | 0,58 | 0,6 | 0,67 | 0,57 | 0,27 | 0,05 | 0,06 | 0,31 |
| Th | 0,12 | 0,09 | 0,15 | 0,26 | 0,2 | 0,87 | 0,12 | 0,3 | 0,38 | 0,2 | 0,35 | 0,92 | 0,03 | 0 | 0,33 |
| Tm | 0,26 | 0,23 | 0,14 | 0,32 | 0,12 | 0,17 | 0,5 | 0,28 | 0,31 | 0,34 | 0,28 | 0,14 | 0,04 | 0,05 | 0,17 |
| U | 0,06 | 0,06 | 0,08 | 0,13 | 0,12 | 0,41 | 0,07 | 0,13 | 0,14 | 0,08 | 0,17 | 0,35 | tr | tr | 0,37 |
| V | 231,2 | 382,4 | 231,1 | 240,4 | 250,2 | 67,65 | 189,7 | 209,1 | 192,4 | 547,4 | 172,5 | 227,1 | 62,7 | 101 | 181,08 |
| Y | 17,53 | 15,56 | 9,07 | 21,06 | 8,49 | 11,74 | 31,9 | 18,33 | 19,44 | 22,3 | 17,85 | 9,61 | 2,66 | 3,24 | 10,56 |
| Yb | 1,69 | 1,46 | 0,87 | 1,95 | 0,78 | 1,07 | 3,26 | 1,76 | 1,91 | 2,13 | 1,74 | 0,98 | 0,23 | 0,35 | 1,10 |
| Zr | 27,38 | 25,55 | 15,14 | 34,72 | 18,3 | 21,31 | 33,44 | 23,82 | 27,9 | 30,68 | 23,41 | 36,34 | 6,22 | 6,03 | 40,20 |

These characteristics are comparable to those of some basic to ultrabasic Pogwa (Table 1) and Ladanka (Table 2) plutonites highlighted in the Diagorou-Darbani greenstone belt of Niger's Liptako by Soumaila et al. (2016a, 2016b). This suggests that these enclaves come from the plutonites that the pluton ripped out when it was being set up.

Table 2 : Majors and trace elements analyses of the Ladanka Rocks (Soumaila et al.,2016b)

| Rocks | Soumaila et al., 2016b | | | | | | | | | | | | |
|--------------------------------|------------------------|---------|--------|-------------------|--------|--------|--------|--------|--------|--------|--------|--------|------------------|
| | Ultrabasic | | | Metagabbro massif | | | | | | | | | Metagabbro lited |
| Samples | Fpd-26a | Fpd-26b | Fpd-25 | Fpd-31 | Fpd-33 | Fpd-27 | Fpd-28 | Fpd-32 | Fpd-34 | Fpd-35 | Fpd-36 | Fpd-29 | Fpd-30 |
| SiO ₂ | 43,92 | 44,4 | 48,13 | 47,85 | 48,65 | 48,69 | 49,38 | 44,91 | 49,6 | 47,78 | 49,22 | 48,67 | 46,5 |
| Al ₂ O ₃ | 1,39 | 1,61 | 6,58 | 13,99 | 16,55 | 17,62 | 18,56 | 14,87 | 18,1 | 15,84 | 15,87 | 14,05 | 18,76 |
| Fe ₂ O ₃ | 15,05 | 13,78 | 10,31 | 5,65 | 5,93 | 4,76 | 5,83 | 9,66 | 4,99 | 6,94 | 6,74 | 6 | 6,39 |
| MnO | 0,17 | 0,22 | 0,13 | 0,12 | 0,11 | 0,1 | 0,11 | 0,14 | 0,1 | 0,12 | 0,12 | 0,13 | 0,11 |
| MgO | 24,85 | 23,36 | 29,53 | 12,12 | 9,42 | 9,28 | 9,27 | 14,14 | 10,44 | 10,98 | 10,87 | 10,43 | 9,36 |
| CaO | 8,39 | 12,33 | 3,68 | 16,72 | 15,84 | 16,72 | 14,2 | 11,78 | 14,92 | 14,27 | 13,59 | 17,71 | 15,42 |
| Na ₂ O | 0,05 | - | - | 0,57 | 1,06 | 0,59 | 1,19 | 1,19 | 0,83 | 0,61 | 0,85 | 0,73 | 0,49 |
| K ₂ O | - | - | - | - | - | - | - | - | - | - | - | - | - |
| TiO ₂ | 0,19 | 0,29 | 0,15 | 0,16 | 0,2 | 0,11 | 0,12 | 0,1 | 0,11 | 0,14 | 0,13 | 0,25 | 0,13 |
| P ₂ O ₅ | - | - | - | - | - | 0,05 | - | - | - | - | - | - | 0,05 |
| Total | 100,03 | 99,61 | 100,14 | 99,55 | 99,86 | 99,87 | 99,78 | 99,89 | 99,93 | 99,01 | 99,8 | 99,41 | 99,9 |
| Ba | 10,28 | 21,57 | 3,4 | 110,1 | 53,43 | 32,74 | 31,86 | 31,56 | 21,18 | 15,78 | 33,82 | 27,9 | 10,45 |
| Ce | 1,1 | 1,19 | 1,81 | 1,01 | 0,86 | 1,73 | 1,17 | 0,98 | 1,14 | 1,37 | 1,33 | 1,93 | 1,53 |
| Co | 109,2 | 107,3 | 90,98 | 41,63 | 39,01 | 35,16 | 39,49 | 72,21 | 35,35 | 53,57 | 43,91 | 36,21 | 44,45 |
| Cr | 1332 | 1647 | 3179 | 922 | 571 | 810 | 126 | 897 | 382 | 983 | 271 | 647 | 435 |
| Dy | 0,99 | 1,26 | 0,77 | 0,92 | 0,83 | 0,73 | 0,58 | 0,59 | 0,51 | 0,62 | 0,55 | 1,16 | 0,6 |
| Er | 0,58 | 0,71 | 0,5 | 0,55 | 0,54 | 0,46 | 0,37 | 0,36 | 0,33 | 0,39 | 0,35 | 0,65 | 0,36 |
| Eu | 0,14 | 0,31 | 0,13 | 0,27 | 0,28 | 0,23 | 0,26 | 0,22 | 0,22 | 0,23 | 0,23 | 0,4 | 0,25 |
| Gd | 0,89 | 1,07 | 0,63 | 0,73 | 0,64 | 0,6 | 0,48 | 0,45 | 0,42 | 0,51 | 0,45 | 1,06 | 0,47 |
| Hf | 0,18 | 0,21 | 0,26 | 0,12 | 0,12 | 0,12 | 0,1 | 0,11 | 0,12 | 0,1 | 0,09 | 0,23 | 0,1 |
| Ho | 0,21 | 0,26 | 0,17 | 0,19 | 0,18 | 0,16 | 0,12 | 0,13 | 0,12 | 0,13 | 0,12 | 0,24 | 0,13 |
| La | 0,28 | 0,27 | 0,64 | 0,71 | 0,34 | 1,87 | 0,48 | 0,48 | 0,47 | 0,99 | 0,6 | 0,77 | 1,3 |
| Lu | 0,09 | 0,1 | 0,08 | 0,08 | 0,08 | 0,07 | 0,06 | 0,06 | 0,05 | 0,06 | 0,06 | 0,09 | 0,06 |
| Nb | 0,13 | - | 0,36 | - | - | 0,11 | - | - | - | - | - | - | - |
| Nd | 1,68 | 1,87 | 1,49 | 1,34 | 1,01 | 1,67 | 0,99 | 0,88 | 0,96 | 1,38 | 1,19 | 2,36 | 1,43 |
| mg | 0,65 | 0,65 | 0,76 | 0,7 | 0,64 | 0,68 | 0,64 | 0,62 | 0,7 | 0,64 | 0,64 | 0,66 | 0,62 |

| | | | | | | | | | | | | | |
|----|------|------|------|------|------|------|------|------|------|------|------|------|------|
| Ni | 646 | 627 | 1290 | 235 | 154 | 156 | 137 | 333 | 204 | 199 | 139 | 141 | 113 |
| Pb | - | - | - | - | - | 1,95 | - | - | - | - | - | - | - |
| Pr | 0,24 | 0,28 | 0,3 | 0,24 | 0,17 | 0,39 | 0,19 | 0,17 | 0,18 | 0,28 | 0,23 | 0,41 | 0,34 |
| Rb | - | - | - | 1,51 | 1,54 | 1,03 | 0,87 | 2,91 | - | 0,81 | 1,12 | 1,09 | - |
| Sm | 0,7 | 0,77 | 0,5 | 0,5 | 0,43 | 0,44 | 0,35 | 0,32 | 0,31 | 0,39 | 0,39 | 0,85 | 0,39 |
| Sr | 8 | 11 | 17 | 162 | 166 | 165 | 238 | 149 | 226 | 224 | 196 | 257 | 205 |
| Ta | - | - | 0,03 | - | - | - | - | - | - | - | - | - | - |
| Tb | 0,15 | 0,19 | 0,12 | 0,13 | 0,12 | 0,11 | 0,08 | 0,08 | 0,08 | 0,09 | 0,08 | 0,18 | 0,09 |
| Th | 0,07 | - | 0,05 | - | - | 0,09 | - | - | - | - | - | - | 0,24 |
| Tm | 0,09 | 0,11 | 0,08 | 0,08 | 0,08 | 0,07 | 0,06 | 0,05 | 0,05 | 0,06 | 0,06 | 0,09 | 0,06 |
| U | 0,05 | - | - | - | - | 0,08 | - | - | - | - | - | - | - |
| V | 137 | 166 | 111 | 132 | 144 | 129 | 97 | 94 | 92 | 129 | 132 | 153 | 103 |
| Y | 5,43 | 6,76 | 4,6 | 5,39 | 5,34 | 4,54 | 3,36 | 3,57 | 3 | 3,75 | 3,29 | 6,23 | 3,33 |
| Yb | 0,58 | 0,68 | 0,52 | 0,52 | 0,53 | 0,45 | 0,37 | 0,37 | 0,33 | 0,38 | 0,38 | 0,6 | 0,38 |
| Zr | 3,77 | 4,19 | 8,93 | 2,62 | 2,78 | 3,67 | 2,53 | 2,89 | 2,54 | 2,75 | 2,29 | 4,28 | 2,08 |

The basic to ultrabasic plutonites of Pogwa and Ladanka correspond to meta-ultrabasites (serpentinites), metapyroxenites, garnet-bearing amphibolites, and massive or locally bedded metagabbros (massive amphibolites) (Soumaila et al., 2016a, 2016b). These plutonites have high levels of MgO, Ni, and Cr, and are depleted in light rare earths (Soumaila et al., 2016a, 2016b). These plutonites were considered to be the plutonic base unit of a N-MORB ocean floor with an oceanic plateau, having been influenced to a greater or lesser extent by an oceanic arc (Soumaila et al., 2016a, 2016b). These rocks result from the fractional crystallization of a magmatic liquid from a mantle source depleted by partial melting cycles at variable rates (ultrabasites: 80%, basics: 20 to 40%) (Soumaila et al., 2016b). Soumaila et al. (2016a, 2016b) have determined the environment and mode of emplacement of basic to ultrabasic plutonites without determining the nature of the magmatic lineage of these rocks.

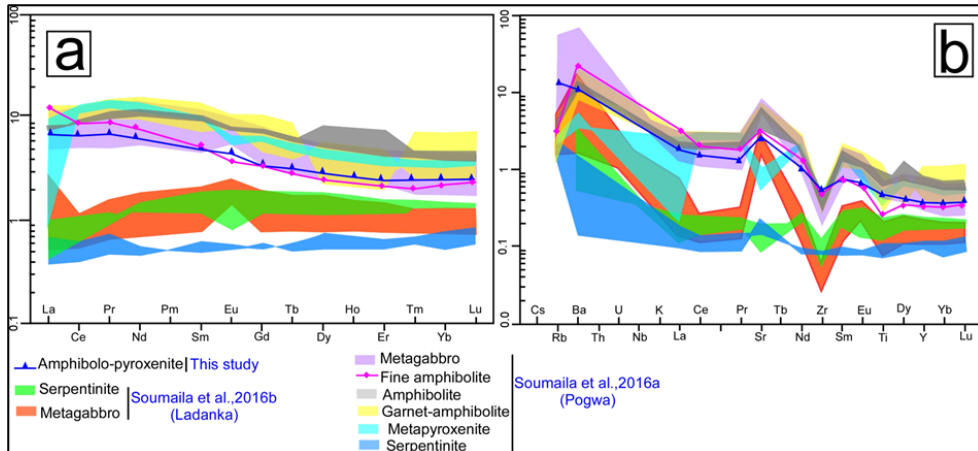


Figure 6: (a) Rare-earth spectra of the amphibolo-pyroxenite enclave and the basic to ultrabasic plutonites normalized to the primitive mantle of McDonough and Sun (1995) ; (b) Multi-element spectra of the amphibolo-pyroxenite enclave and the basic to ultrabasic plutonites normalized to the NMORB of Sun and McDonough (1989)

These basic plutonites to ultrabasites have signatures different from those of most of the tholeiitic and calc-alkaline birimian basites of the West African Craton (Abouchami et al., 1990; Boher et al., 1992). According to the authors, the tholeiitic lineage characterizes an emplacement in a MORB-type oceanic domain (Lompo, 2009), an oceanic shelf area (Poucllet et al., 1996), or an island arc domain (Ama Salah et al., 1996; Soumaila et al., 2004, 2008). The calc-alkaline lineage characterizes an emplacement in a subduction context (Ama Salah et al., 1996; Soumaila et al., 2004, 2008).

The projection of the amphibolo-pyroxenite enclave and the basic to ultrabasic plutonites in the Jensen (1976) (Figure 7) shows that the amphibolo-pyroxenite enclave of the Téra Ayorou pluton and some basic to ultrabasic plutonites of the Diagorou-Darbani greenstone belt fall within the komatiite field. This diagram shows that the metapyroxenites, amphibolites, and amphibolo-pyroxenites are komatiitic basalts, while the serpentinites are komatiites. This suggests that the amphibolo-pyroxenite enclaves of the Téra-Ayorou pluton and some basic to ultrabasic plutonites of the Diagorou-Darbani greenstone belt constitute a fairly continuous komatiitic line of rocks from peridotites (serpentinites) to basalts (metapyroxenites, amphibolites). This komatiitic lineage is different from the tholeiitic and calc-alkaline lineages with which it is closely intertwined in the field.

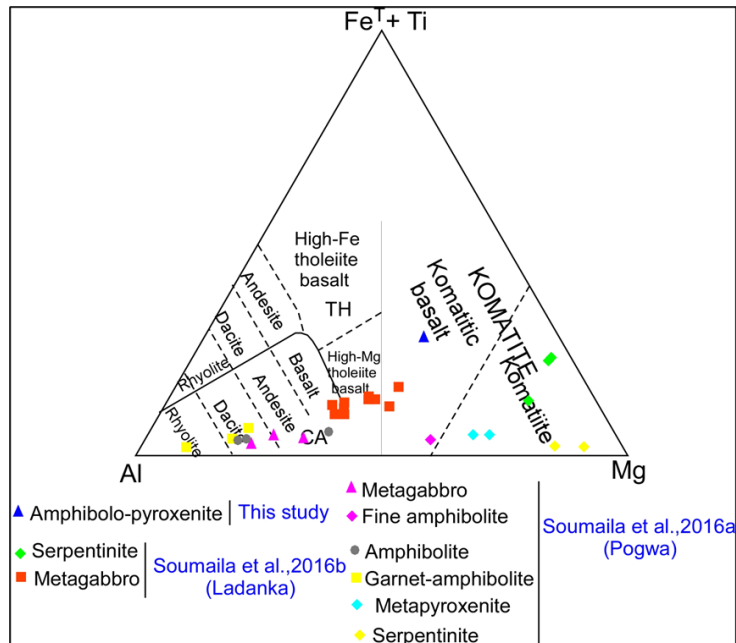


Figure 7: Projection of the amphibolo-pyroxenite enclave of the Téra-Ayorou (this study) and the basic to ultrabasic plutonites of the Diagorou-Darbani belt (Soumaila et al., 2016a, 2016b) in the Jensen (1976) diagram

At the scale of the West African Craton, the basic to ultrabasic enclaves of the Tera-Ayorou pluton are comparable to the mafic to ultramafic Birimian rocks of komatiitic affinity of the Boromo (Burkina-Faso) (Aïfa, 2021), Kotiala-Marbadissa (Ivory Coast) (Doumbia et al., 1998; Pouclet et al., 2006; Aïfa, 2021) and the Niandan belt (Guinea) (Milési et al., 1989; Tegye and Johan, 1989; Grenholm, 2019). These enclaves of the Tera-Ayorou pluton are also comparable to the mafic to ultramafic rocks of the Paleoproterozoic belt of the Paramaca (Guyana) (Marot and Capdevila, 1980; Milési and Picot, 1995; Capdevila et al., 1999).

Conclusion

The enclaves of amphibolites, pyroxenites, and amphibolo-pyroxenites in the Téra-Ayorou pluton are composed of quartz, plagioclase, pyroxene, and hornblende. These basic rock enclaves are characterized by high levels of MgO, low levels of Na₂O, K₂O and TiO₂, high CaO/Al₂O₃ ratios, depletion of light rare earths, and enrichment in Ni and Cr. These enclaves have a geochemical affinity that is very similar to that of the basic to ultrabasic Pogwa and Ladanka plutonites of the Diagorou-Darbani greenstone belt. This suggests that these enclaves were ripped out by the pluton as it was being emplaced. The amphibolo-pyroxenite enclaves of the Téra-Ayorou pluton and the basic to ultrabasic plutonites of the Diagorou-Darbani

greenstone belt constitute a fairly continuous komatiitic affinity line of rocks from peridotites (serpentinites) to basalts (metapyroxenites, amphibolites). This komatiitic lineage is thought to result from the fractional crystallization of a magmatic liquid from a mantle source depleted by cycles of partial melting at variable rates.

Conflict of Interest: The authors reported no conflict of interest.

Data Availability: All data are included in the content of the paper.

Funding Statement: The authors did not obtain any funding for this research.

References:

1. Abouchami, W., Boher, M., Michard, A., and Albarede, F. (1990). A Major 2.1 Ga event of mafic magmatism in west Africa: An early stage of Crustal accretion: *Journal of Geophysical Research*, p. 17605–17629.
2. Ahmed, Y.L., Attourabi, S.A., Hallarou, M.M., Chamsi, L.I., Noura, G.R., and Chékaraou, M.M.S. (2022). Relationship between regional deformation and the emplacement of the Dibilo pegmatites (Liptako, West Niger): *Journal of African Earth Sciences*, v. 198, p. 1–16, doi: <https://doi.org/10.1016/j.jafrearsci.2022.104814>.
3. Aïfa, T. (2021). Mineralization and sustainable development in the West African Craton: from field observations to modelling: Geological Society, London, Special Publications, p. 1–29, doi: <https://doi.org/10.1144/SP502-2021-21>.
4. Ama Salah, I., Liegeois, J.P., and Pouclet, A. (1996). Evolution d'un arc insulaire océanique birimien précoce au Liptako nigérien (Sirba) : géologie, géochronologie et géochimie: *Journal of African Sciences*, v. 22, p. 235–254.
5. Attourabi, S.A., Ahmed, Y.L., and Hallarou, M.M. (2021). Origin and emplacement conditions of the Dibilo lithiniferous mineralization (Liptako, Western Niger): *International Journal of Science and Research (IJSR)*, v. 10, p. 55–71, doi:10.21275/SR21917211430.
6. Baratoux, L., Metelka, V., Naba, S., Jessell, M.W., Grégoire, M., and Ganne, J. (2011). Juvenile Paleoproterozoic crust evolution during the Eburnean orogeny (2.2–2.0 Ga), western Burkina Faso: *Precambrian Research*, v. 191, p. 18–45.
7. Baratoux, L., Metelka, V., Naba, S., Ouyi, P., Siebenaller, L., Jessell, M.W., Naré, A., Salvi, S., Béziat, D., and Franceschi, G. (2015). Tectonic evolution of the Gaoua region, Burkina Faso: Implications

- for mineralization: *Journal of African Earth Sciences*, v. 112, p. 419–439.
8. Blais, S., Auvray, B., Capdevila, R., Hameurt, J. (1977). Les séries komatiitiques et tholéitiques des ceintures archéennes de roches vertes de Finlande orientale: *Bull. Soc. géol. France.*, v7, t XIX.n°5, 965-970.
 9. Boher, M., Abouchami, W., Michard, A., Albarede, F., and Arndt, N.T. (1992). Crustal growth in West Africa at 2.1 Ga: *J. Géophys.*, v. 97, p. 345–369.
 10. Capdevila, R., Arndt, N., Letendre, J., and Sauvage, J.-F. (1999). Diamonds in volcanoclastic komatiite from French Guiana: *Nature*, v. 399, p. 456–458.
 11. Cheilletz, A., Babey, P., Lama, C., Pons, J., Zimmermann, J.-L., and Dautel, D. (1994). Age de refroidissement de la croûte juvénile birimienne d’Afrique de l’Ouest, Données U/Pb et K-Ar sur les formations à 2.1Ga du SW du Niger: *Comptes Rendus de l’Académie des Sciences, Paris, Série II*, v. 319, p. 435–442.
 12. Doumbia, S., Pouclet, A., Kouamelan, A.N., Peucat, J.J., Vidal, M., and Delor, C. (1998). Petrogenesis of juvenile-type Birimian Paleoproterozoic granitoids in central Côte-d’Ivoire, West Africa: geochemistry and geochronology: *Precambrian Research*, v. 87, p. 33–63.
 13. Dupuis, D., Pons, J., and Prost, A.E. (1991). Mise en place de plutons et caractérisation de la déformation birimiène au Niger Occidental: *Comptes Rendus de l’Académie des Sciences, Paris*, v. 312, p. 769–776.
 14. Garba Saley, H., Konate, M., and Soumaila, A. (2021). Étude texturale des chromitites paléoprotérozoïques de la Région de Makalondi, Province du Liptako nigérien, Ouest Niger : Origine et condition de mise en place: *Afrique SCIENCE*, v. 18, p. 186–202.
 15. Grenholm, M. (2019). The global tectonic context of the ca. 2.27-1.96 Ga Birimian Orogen—Insights from comparative studies, with implications for supercontinent cycles: *Earth-science reviews*.
 16. Hallarou, M.M. (2021). Contexte de mise en place des minéralisations en cuivre et en molybdène des formations Birimiennes de la région de Kourki (Liptako, Ouest Niger) : Genèse et Evolution Magmatique [Thèse de Doctorat Unique]: Université Abdou Moumouni de Niamey, 255 p.
 17. Janoušek, V., Colin, M.F., and Vojtech, E. (2006). Interpretation of whole-rock geochemical data in igneous geochemistry: introducing Geochemical Data Toolkit (GCDkit): *Journal of Petrology*, v. 47, p. 1255–1259.

18. Jensen, L.S. (1976). A New Cation Plot for Classifying Subalkalic Volcanic Rocks: Ontario Geological Survey Miscellaneous Paper 66.
19. Kouamelan, A.N., Djro, S.C., and Allialy, M.E. (2015). The oldest rock of Ivory Coast: *Journal of African Earth Sciences*, v. 103, p. 65–70, doi: 10.1016/j.jafrearsci.2014.12.004.
20. Lama, C. (1993), Apport de la Méthode K-Ar a la compréhension de l'histoire géologique des granitoïdes birimiens du Liptako (Niger Occidental) et des leucogranites a 2 micas de Tagragra d'Akka (Anti-Atlas Occidental, Maroc) [Thèse INPL]: Université de Lorraine, 142 p.
21. Lompo, M. (2009). Geodynamic evolution of the 2.25-2.0 Ga Palaeoproterozoic magmatic rocks in the Man-Leo Shield of the West African Craton. A model of subsidence of an oceanic plateau: *Geological Society, London, Special Publications*, v. 323, p. 231–254.
22. Machens, E. (1973). Contribution à l'étude des formations du socle cristallin et de la couverture sédimentaire de l'Ouest de la République du Niger.: *Mémo. BRGM*, n° 82, 167 p.
23. Machens, E. (1961). Prospection Générale du Liptako, campagne 1960-1961. *B.R.G.M.*: 73 p.
24. Marot, A., and Capdevila, R. (1980). Géologie du synclinorium du Sud de la Guyane française: 9a Conferencia Geologica del Caribe, Sano Domingo, Republica Dominicana, *Memorias*, v. 2, p. 613–618.
25. McDonough, W.F., and Sun, S.S. (1995). The composition of the Earth: *Chem. Geol*, v. 120, p. 223–253, doi: [https://doi.org/10.1016/0009-2541\(94\)00140-4](https://doi.org/10.1016/0009-2541(94)00140-4).
26. Milési, J.P. et al. (1989). Les minéralisations aurifères de l'Afrique de l'Ouest. Leurs relations avec l'évolution lithostructurale au Protérozoïque inférieur: *Chronique de la Recherche Minière*, n° 497, p. 3–98.
27. Milési, J.P., and Picot, J.C. (1995). L'or en Guyane française: contexte et potentiel géologiques: *Rap. BRGM R 38517*, p. 1–31.
28. Noura, G.R., Ahmed, Y.L., Baratoux, L., Ernst, R.E., Attourabi, S.A., Hallarou, M.M., Chamsi, L.I., and Chékaraou, M.M.S. (2023a). Petrogenesis and geochemistry of WNW-ESE to NW-SE trending doleritic dykes of the Paleoproterozoic Liptako basement (West African Craton, West Niger): *Journal of African Earth Sciences*, v. 208, p. 1–17, doi:<https://doi.org/10.1016/j.jafrearsci.2023.105096>.
29. Parra-Avila, L.A. et al. (2017). The geochronological evolution of the Paleoproterozoic Baoulé-Mossi domain of the Southern West African Craton: *Precambrian Research*, v. 300, p. 1–27.
30. Pons, J., Barbey, P., Dupuis, D., and Leger, J.M. (1995). Mechanisms of pluton emplacement and structural evolution of a 2.1 Ga juvenile

- continental crust: the Birimian of southwestern Niger: *Precambrian Research*, v. 70, p. 281–301.
31. Pouclet, A., Doumbia, S., and Vidal, M. (2006). Geodynamic setting of the Birimian volcanism in central Ivory Coast (western Africa) and its place in the Palaeoproterozoic evolution of the Man Shield: *Bull. Soc. Géol. Fr*, v. 177, p. 105–121.
 32. Pouclet, A., Vidal, M., Delor, C., Simeon, Y., and Alric, G. (1996). Le volcanisme birimien du Nord-Est de la Côte-d'Ivoire : mise en évidence de deux phases volcano-tectoniques distinctes dans l'évolution géodynamique du Paléoprotérozoïque: *Bull. Soc. Géol. Fr*, v. 167, p. 529–541.
 33. Rollinson, H. (2016). Archaean crustal evolution in West Africa: A new synthesis of the Archaean geology in Sierra Leone, Liberia, Guinea and Ivory Coast: *Precambrian Research*, v. 281, p. 1–12.
 34. Soumaila, A., Ahmed, Y.L., and Nouhou, H. (2016b). Géochimie des basites et ultrabasites de Ladanka (Liptako, Niger): *J.Sci*, v. 16, p. 37–54.
 35. Soumaila, A., Garba, Z., Moussa, I.A., Nouhou, H., and Sebag, D. (2016a). Highlighting the root of a paleoproterozoic oceanic arc in Liptako, Niger, West Africa: *Journal of Geology and Mining Research*, v. 8, p. 13–27, doi:10.5897/JGMR2015.0230.
 36. Soumaila, A., Henry, P., Garba, Z., and Rossi, M. (2008). REE patterns, Nd-Sm and U-Pb ages of the metamorphic rocks of the Diagorou-Darbani greenstone belt (Liptako, SW Niger): implication for Birimian (Palaeoproterozoic) crustal genesis: *Geological Society, London, Special Publications*, p. 19–32, doi:10.1144/SP297.2.
 37. Soumaila, A., Henry, P., and Rossy, M. (2004). Contexte de mise en place des roches basiques de la ceinture de roches vertes birimienne de Diagorou-Darbani (Liptako, Niger, Afrique de l'Ouest): plateau océanique ou environnement d'arc/bassin arrière-arc océanique: *C. R. Geoscience*, n° 336, p. 1137–1147.
 38. Sun, S.S., and McDonough, W.F. (1989). Chemical and isotopic systematics of oceanic basalts: implications for mantle composition and processes. In: Saunders, A.D. and Norry, M.J. (eds), *Magmatism in ocean basins: Geological Society, London, Special Publications*, p. 313–345.
 39. Tegye, M., and Johan, V. (1989). Une séquence komatiitique dans le Protérozoïque inférieur de Guinée (Afrique de l'Ouest): Caractères pétrographiques, minéralogiques et géochimiques: *Comptes Rendus de l'Académie des Sciences, Paris . Série 2, Mécanique, physique, chimie, sciences de l'univers, sciences de la terre*, p. 1984–1993.